J Mater Sci (2007) 42:9037–9044
DOI 10.1007/s10853-007-1819-z

Study of air oxidation of amorphous $Zr_{65}Cu_{17.5}Ni_{10}Al_{7.5}$ by X-ray photoelectron spectroscopy (XPS)

A. Dhawan · V. Zaporojtchenko · F. Faupel · S. K. Sharma

Received: 2 April 2007 / Accepted: 2 May 2007 / Published online: 20 July 2007

Abstract The oxidation of the bulk amorphous alloy $Zr_{65}Cu_{17.5}Ni_{10}Al_{7.5}$ in air in its amorphous and the supercooled liquid states was studied in the temperature range 573–663 K using X-ray photoelectron spectroscopy (XPS). The oxide film mainly consisted of the oxides of Zr (as ZrO_2) and Al (as Al_2O_3). No Cu or Ni was found in the oxide film formed on the amorphous state of the alloy while significant Cu (as CuO) was present in the oxide film formed on the alloy in its supercooled liquid state. The role of the various alloying elements during oxidation at high temperatures in air is discussed in the paper. The XPS data from oxide film support the previously suggested mechanism for oxidation of this alloy, i.e. the rate controlling process during oxidation of the alloy at low temperatures (in the amorphous state) is the back-diffusion of Ni and Cu, while the oxidation at high temperatures (in the supercooled liquid state) is dominated by the inward diffusion of oxygen.

Introduction

Bulk amorphous alloys show a fairly wide temperature range between glass transition and the crystallization temperature and a remarkable resistance to crystallization. The bulk metallic glasses require cooling rates of about 1–100 K/s or less unlike conventional melt-spun metallic glasses which require very high cooling rates of about 10^6 K/s for processing [1]. The interest in bulk amorphous glasses has considerably grown in recent times due to their ability to offer the scope for carrying out research investigations both in the amorphous and the supercooled liquid states of a glassy alloy. Novel multicomponent Zr-based alloys like Zr–Ti–Cu–Ni–Be and Zr–Cu–Ni–Al form an important class of bulk metallic glasses with some interesting applications [2].

In contrast to several studies done on the oxidation behaviour of conventional melt-spun amorphous alloys [3–7 references therein], not many studies are available on oxidation of bulk metallic glasses [8–16]. In one of the early investigations on high temperature oxidation of the bulk amorphous alloy $Zr_{60}Al_{15}Ni_{25}$ in air it was suggested that the growth of the oxide is controlled by Ni back-diffusion in the alloy [11]. Contrary to these observations Triwikantoro et al. [12] investigated the oxidation of several Zr-based amorphous alloys (Zr–Cu–Ni–Al) in air and reported the presence of Cu and Ni in the oxide scale. In another investigation by the present authors on oxidation of the bulk amorphous alloy $Zr_{65}Cu_{17.5}Ni_{10}Al_{7.5}$ [14], a mechanism for its oxidation in air was proposed suggesting that the back diffusion of Ni, and possibly Cu also, is the rate limiting process during the oxidation of the alloy in the amorphous or the glassy state, while oxidation process in the supercooled liquid state is more likely dominated by the diffusion of oxygen through the oxide layer [14]. In order to verify this suggested mechanism, it is necessary to obtain information about the presence of various alloy constituents, especially Ni and Cu, in the oxide film using some depth profiling technique. This was a motivating

A. Dhawan · S. K. Sharma (✉)
Department of Physics, Malaviya National Institute of Technology, Jaipur 302 017, India
e-mail: sksh@datainfosys.net

V. Zaporojtchenko · F. Faupel
Faculty of Engineering, University of Kiel, Kaiserstr. 2, 24143 Kiel, Germany

Present Address:
A. Dhawan
Department of Physics, Jagannath Gupta Institute of Engineering & Technology, Jaipur 302 022, India

factor for carrying out the present investigations. The technique of X-ray photoelectron spectroscopy (XPS) was employed in conjunction with Ar^+ ion sputtering for obtaining the desired information from the oxide film formed on amorphous and supercooled liquid states of the bulk alloy $Zr_{65}Cu_{17.5}Ni_{10}Al_{7.5}$ during its oxidation in air in the temperature range 573–663 K.

Experimental

Specimens of size (10 mm × 15 mm) were cut from the as-cast amorphous ribbon (10 mm wide × 30 μm thick) of the bulk amorphous alloys $Zr_{65}Cu_{17.5}Ni_{10}Al_{7.5}$. The samples were first cleaned ultrasonically in acetone and ethanol and later dried under a jet of pressurised air. These samples were put in an open-ended quartz tube which was inserted in a tubular furnace and annealings were performed at 573 K for 20 h, 603 K for 8 h, 633 K for 3 h and 663 K for 1 h in dry air environment inside the open-ended quartz tube. As the oxidation was carried out ex-situ in a furnace it was not possible to remove the native oxide layer from the specimens by carrying out ion beam sputter cleaning or scribing in a vacuum chamber. The study of the native oxide formed on this alloy has earlier been reported in another investigation [9]. The choice of time–temperature combination for annealing was made on the basis of the results obtained in our previous investigation [14] and the known T–T–T diagram for this alloy [17, 18] so that the alloy $Zr_{65}Cu_{17.5}Ni_{10}Al_{7.5}$ remained after oxidation treatment either in the amorphous (573 and 603 K) or in the supercooled liquid state (633 and 663 K) and did not crystallize during annealing. Then the annealed samples were taken out of the furnace and the shiny side (free surface during melt- spinning of the alloy) was analysed by X-ray photoelectron spectroscopy (XPS). The XPS measurements were done using an electron spectrometer (VG MK II) equipped with a non-monochromatic Mg K_α source energy ($h\nu$ = 1253.6 eV) in a base pressure better than 1.0×10^{-10} m-bar in the analysis chamber and a hemispherical electron analyser at a pass energy of 50 eV. XPS peaks for constituent elements: Zr 3d, Al 2s, Cu 2p and Ni 2p were recorded along with the XPS peaks for O 1s and C 1s. The sub-surface layers in oxide films were analysed by performing sequential sputtering using argon ions (Ar^+) of 5.0 keV energy. A typical mean sputtering rate of 0.71 nm/min was obtained at this energy of argon ions (Ar^+) on the basis of sputter-rate versus depth scale calibration measurements. The surface morphology of alloy specimens after oxidation was observed with a scanning electron microscope (SEM, FEI Quanta) operating at 30 kV.

Results and discussion

The oxide films formed on the alloy surface as a result of high temperature (in the temperature range 573–663 K) oxidation in air were characterized by XPS. The main features of XPS peaks from specimens annealed at 573 and 603 K (corresponding to the oxidation of specimens in the amorphous state) were quite similar. Similar observations were made from XPS peaks obtained from specimens annealed at 633 and 663 K (corresponding to the oxidation of specimens in the supercooled liquid state). Therefore, the figures at two typical temperatures 573 and 633 K which correspond to oxidation of specimens in the amorphous and the supercooled liquid states of the alloy, respectively, are shown here and discussed in the following.

Figure 1 depicts the Zr 3d spectra recorded from the oxide films formed on specimens of amorphous $Zr_{65}Cu_{17.5}Ni_{10}Al_{7.5}$ at temperatures 573 and 633 K for the as-received specimens and after sputtering with 5 keV Ar^+ ions. The XPS peaks for Zr 3d are reported to occur at 178.7 and 182.2 eV for Zr^0 (in metallic form) and Zr^{4+} (in oxide form), respectively [19]. Therefore, the Zr 3d XPS peaks in Fig. 1a and b occurring at 181.9 eV and 182.4 eV for the specimen oxidized at 573 K from the as-received and the sputtered specimen surface, respectively and also the corresponding XPS peaks (c) and (d) in the same figure occurring at 182.0 and 182.5 eV for oxidation at 633 K, are suggestive of the presence of Zr^{4+} species on the top surface [9, 19–21]. A small shift of about 0.5 eV in Zr 3d peak towards higher binding energy side after sputtering , i.e. after removal of the adsorbed hydrocarbon impurity layer after argon ion sputtering, may be attributed to chemical

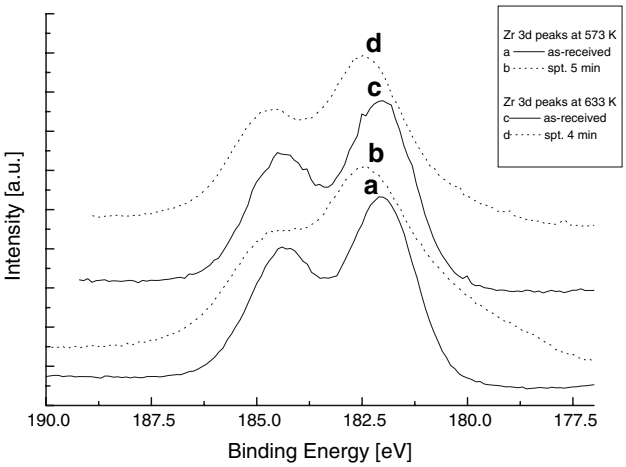

Fig. 1 XPS peaks for Zr 3d from specimens of amorphous $Zr_{65}Cu_{17.5}Ni_{10}Al_{7.5}$ after oxidation at 573 K: (a) as-received, (b) after 5 min sputtering; and after oxidation at 633 K: (c) as-received, (d) after 4 min sputtering

binding effects in the multicomponent amorphous alloy [9, 20, 22].

Figures 2 and 3 represent Cu 2p and Ni 2p XPS peaks, respectively. The oxide film formed at 633 K seems to contain significant amount of Cu as is evident from Fig. 2c and d. On the other hand the poor signals of Cu 2p peaks recorded from the specimen surface (Fig. 2a, b) oxidized at 573 K indicate hardly any presence of Cu. The Cu 2p peak in Fig. 2c occurs at 933.6 eV from the as-received amorphous specimen $Zr_{65}Cu_{17.5}Ni_{10}Al_{7.5}$ oxidized at 633 K indicating the presence of Cu^{2+}, possibly as CuO [19]. After sputtering for 4 min with Ar^+ ions, the Cu $2p_{3/2}$ peak (Fig. 2d) shifts to the lower binding energy side, i.e. 932.5 eV indicating the reduction of oxidized copper (Cu^{2+}) to lower valent states (Cu^+, Cu^0) [22, 23]. It is noteworthy here that the possibility of preferential sputtering and the reduction of the oxides to lower valent states during argon ion sputtering of the oxidised alloy surface is not ruled out [22, 23]. However, the qualitative nature of conclusions derived from observations made in the present study is not changed by these effects. It is further interesting to note from Fig. 3 that hardly any Ni is present as can be inferred from the extremely poor signals in the observed Ni 2p peaks from specimens oxidized at 573 and 633 K. It is worth mentioning here that features for Cu and Ni peaks at 603 and 663 K (figures not shown here) were similar to those at 573 and 633 K, respectively. Figure 4 shows Al 2s XPS peaks recorded from the specimen oxidized at 573 and 633 K. The Al 2s peak (Fig. 4) was recorded instead of the more intense Al 2p peak due to the overlap of the latter with the Cu 3p peak [19]. The Al 2s peaks for oxidic Al^{3+} and metallic Al^0 are known to occur at 119.0 and 117.0 eV, respectively [9, 19]. The Al 2s

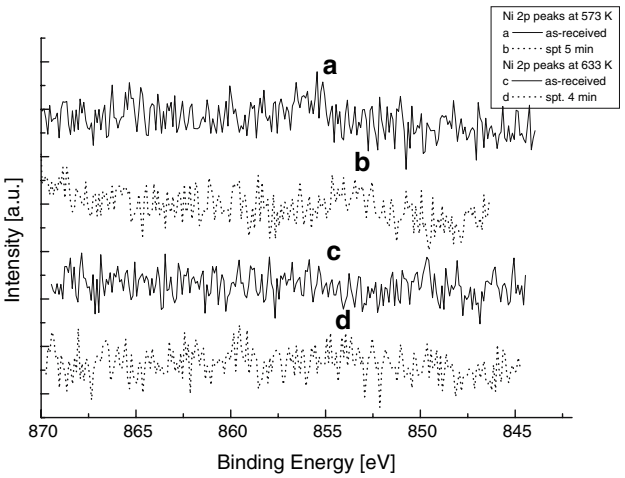

Fig. 3 XPS peaks for Ni 2p from specimens of amorphous $Zr_{65}Cu_{17.5}Ni_{10}Al_{7.5}$ oxidised at 573 K: (a) as-received, (b) after 5 min sputtering; and oxidised at 633 K: (c) as-received, (d) after 4 min sputtering

peaks in Fig. 4 occur about at 119.0 eV in these spectra and thus point to the presence of Al^{3+}, possibly as Al_2O_3 on the surface along with ZrO_2. However, it is interesting to note from this figure that the peak of Al is seen after oxidation at 573 K (Fig. 4a, b) while no significant Al peak is observed after oxidation at 633 K (Fig. 4c, d). A broad peak seen at about 122.0 eV in Fig. 4d stems from Cu 3s [19]. These observations can be understood in conjunction with Cu 2p peaks shown in Fig 2c and d which indicate the presence of significant amount of Cu in the oxide film formed at 633 K and thus the relative concentration of Al in the oxide layer becomes too low to give a significant

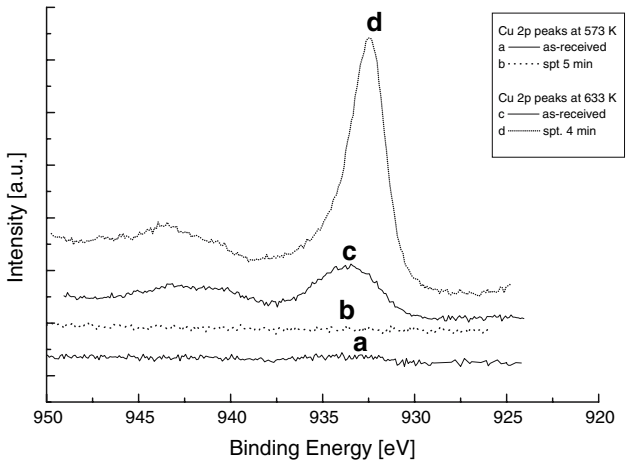

Fig. 2 XPS peaks for Cu 2p from specimens of amorphous $Zr_{65}Cu_{17.5}Ni_{10}Al_{7.5}$ oxidised at 573 K: (a) as-received, (b) after 5 min sputtering; and oxidised at 633 K: (c) as-received, (d) after 4 min sputtering

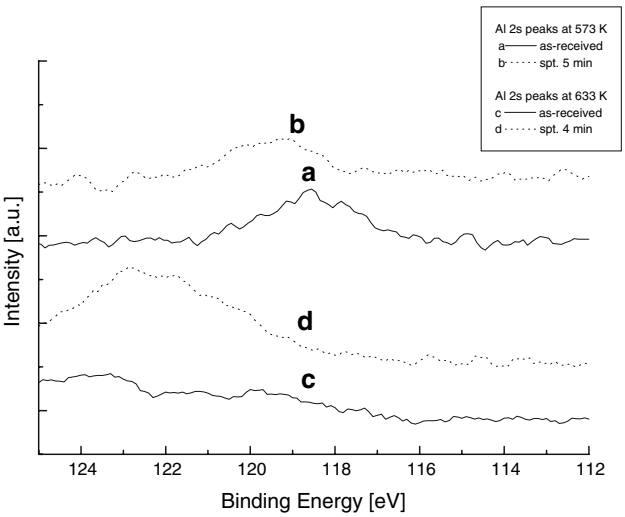

Fig. 4 XPS peaks for Al 2s from specimens of amorphous $Zr_{65}Cu_{17.5}Ni_{10}Al_{7.5}$ oxidised at 573 K: (a) as-received, (b) after 5 min sputtering; and oxidised at 633 K: (c) as-received, (d) after 4 min sputtering

XPS peak of Al from this sample (Fig. 4c, d). It is further interesting to note here that no significant peak due to Cu is seen in the oxide film on the sample oxidised at 573 K (Fig. 2a, b) while Al is present in the oxide film of this sample (Fig. 4a, b). Further, the peak features of Cu and Al peaks after oxidation at 603 and 663 K (figures not shown) were similar to those observed at 573 and 633 K, respectively. Thus from an analysis of Al (Fig. 4) and Cu (Fig. 2) peaks it may be concluded that due to strong segregation of Cu at higher oxidation temperatures (633 and 663 K) the relative amount of Al in the oxide film formed at these temperatures becomes too small to yield significant XPS peaks due to Al. (Fig. 4c, d). This is also evident from Al/Zr depth profile shown in Fig. 7 later.

The formation of various oxides (ZrO_2, CuO, Al_2O_3) is supported by the peak positions of the O 1s peak along with those of the respective alloy constituents (Figs. 1, 2 and 4). Figure 5 depicts the O 1s XPS peaks from oxidized specimens. The O 1s peaks from the as-received surfaces appear at 530.0 eV (Fig. 5a, c) for oxidation at 573 and 633 K, respectively and are shifted to higher binding energy side after sputtering (530.4 eV and 530.6 eV) (Fig. 2b, d). The O 1s peak for oxide formation (O_2^{2-}) has been reported to occur at 530 ± 0.4 eV [9, 19, 20, 24, 25]. The observed asymmetry at high binding energy side in the O 1s curves in Fig. 5a and c before sputtering most likely corresponds to the presence of hydroxyl ions on the surface [9, 19, 20, 25]. This feature disappears after sputtering as is evident from Fig. 5b and d. Therefore, the O 1s spectra shown in Fig. 5 correspond to the formation of oxides of various alloy constituents (ZrO_2, Al_2O_3, CuO) on the top surface at these high temperatures [9, 19, 20, 24, 25]. An understanding about the formation of various oxides on the alloy surface during oxidation in air at various temperatures (in the temperature range 573–663 K) can be obtained from the available values for heat of oxide formation. The heats of formation for ZrO_2, Al_2O_3, NiO and CuO are –1101.1, –1117.6, –497.7 and –314.8 KJ/mol O_2, respectively [26]. This suggests that oxides of Zr and Al in the alloy $Zr_{65}Cu_{17.5}Ni_{10}Al_{7.5}$ are likely to be formed first because of their strong affinity for oxygen, followed by Ni and Cu. However, the back-diffusion or segregation of alloy constituents during oxidation controls the oxidation kinetics and thus the formation of oxidation products in the oxide film.

In the following discussion the role of various alloying elements during oxidation is analysed. It is interesting to note here (Figs. 2 and 3) that hardly any Cu or Ni is seen in the oxide film after oxidation of the alloy at 573 and 603 K (which correspond to the oxidation of the alloy in the amorphous state). However, significant amount of Cu (as CuO) is observed in the oxide film after oxidation at higher temperatures 633 and 663 K (which correspond to the oxidation of the alloy in the supercooled liquid state). On the other hand Al peaks (Fig. 4) show contrasting behaviour with Cu peaks. In order to clearly highlight these observations depth profiles for the concentration ratio of these elements with respect to Zr in the alloy were obtained and are shown in Figs. 6 and 7. An interesting feature of Fig. 6 pertains to the absence of both Cu and Ni in the oxide film formed at 573 and 603 K which correspond to the oxidation of the alloy sample in the amorphous state. In contrast, appreciable amount of Cu is seen in the oxide film formed at 633 and 663 K which correspond to the formation of oxide film in the supercooled liquid state of the alloy. It is interesting to mention here that depth profiles for Al shown in Fig. 7 are in sharp contrast with those for Cu (Fig. 6). Al is present on the surface after oxidation at all temperatures, but hardly any Al is seen deeper in the oxide

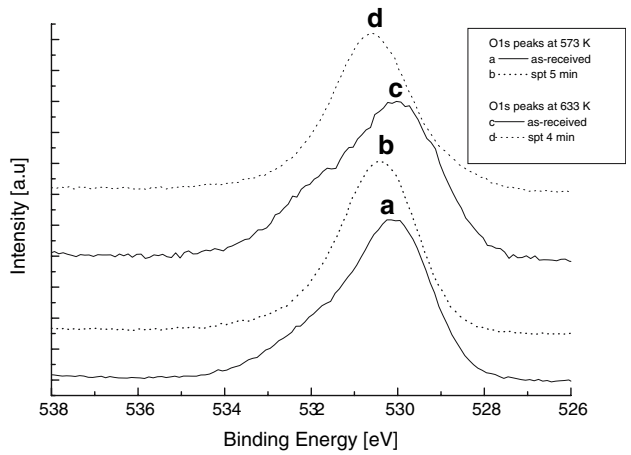

Fig. 5 XPS peaks for O 1s from specimens of amorphous $Zr_{65}Cu_{17.5}Ni_{10}Al_{7.5}$ oxidised at 573 K: (a) as-received, (b) after 5 min sputtering; and oxidised at 633 K: (c) as-received (d) after 4 min sputtering

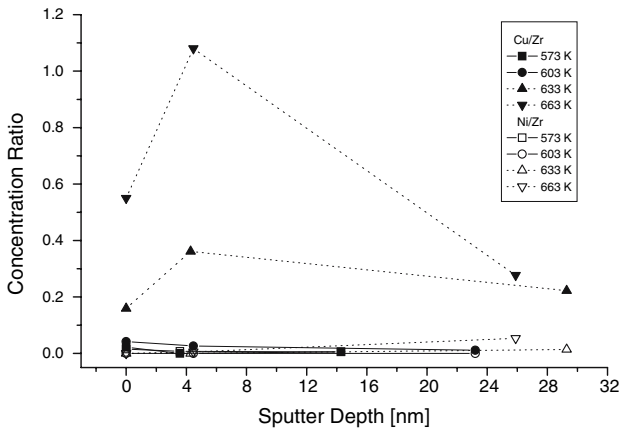

Fig. 6 Plots of atomic concentration ratio [Cu/Zr] and [Ni/Zr] versus sputter depth for the alloy $Zr_{65}Cu_{17.5}Ni_{10}Al_{7.5}$ oxidised at different oxidation temperatures

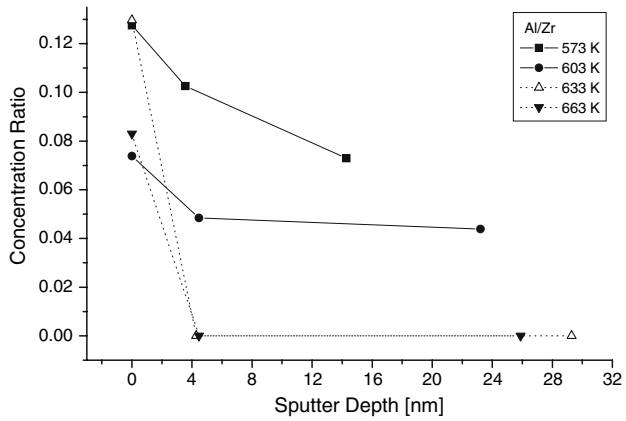

Fig. 7 Plots of atomic concentration ratio [Al/Zr] versus sputter depth for the alloy $Zr_{65}Cu_{17.5}Ni_{10}Al_{7.5}$ oxidised at different oxidation temperatures

film formed at higher temperatures, i.e. at 633 and 663 K (Fig. 7). It is very likely that due to strong segregation of Cu at these temperatures (Fig. 6) the relative concentarion of Al in the oxide film containing Zr and Cu becomes too low to yield a significant XPS peak of Al (Figs. 4 and 7). In fact, Al seen on the surface just at the beginning of the oxidation (see Fig. 7) pertains to the initial amount of Al on the surface, which undergoes oxidation, but its amount is drastically reduced as a result of strong segregation of Cu in the oxide film formed at higher temperatures (Fig. 6). This is supported by the fact that no segregation of Cu is observed during oxidation at 573 and 603 K (Fig. 6) and thus significant amount of Al is seen in the oxide film at these temperatures (Fig. 7). In view of these observations it is suggested that alloy constituents, especially Cu and Ni seem to play an important role during oxidation of the alloy $Zr_{65}Cu_{17.5}Ni_{10}Al_{7.5}$. The role of Cu and Ni is explained by the controlling oxidation mechanisms and is discussed in the following paragraphs.

It was suggested [14] in our previous investigation on oxidation of this alloy that the oxidation in the amorphous state is controlled by the back-diffusion of Ni and Cu while the inward diffusion of oxygen becomes dominant during oxidation of the supercooled liquid state of the alloy. The fact that no Ni and Cu are seen during oxidation of the alloy in its amorphous state clearly supports this mechanism for oxidation of the alloy [14] that the back diffusion of Ni and Cu seems to be the rate controlling process during oxidation of the alloy in its amorphous state. In order to analyse the depth profile in Fig. 6, it would be interesting to get an estimate of the diffusion lengths of these elements using the known diffusivity data [27–29] in this and other similar types of amorphous alloys.

Diffusion rates of Ni in amorphous $Zr_{65}Cu_{17.5}Ni_{10}Al_{7.5}$ are available in the literature [27, 28] while no diffusion data for Cu diffusion in this alloy have so far been reported. An estimate shows that the diffusion length $\sqrt{4Dt}$ of Ni at 573 K is about ~34 nm (D_{Ni} at 573 K = 3.9×10^{-21} m^2/s and t = 20 h, being the time corresponding to the oxidation of the alloy in its amorphous state). A similar calculation at 603 K yields the value of diffusion length as 56 nm (D_{Ni} at 603 K = 2.7×10^{-20} m^2/s and t = 8 h). These estimates are indicative of the fact that due to back diffusion of Ni during oxidation of the alloy specimen in the amorphous state Ni has moved by about 34–56 nm deeper into the alloy beyond the oxide-alloy interface. Though no data for diffusion of Cu in this alloy have been reported in the literature, diffusion of both Cu and Ni have been investigated in another conventional type amorphous alloy $Zr_{50}Cu_{50}$ [29]. The reported data for diffusion of Ni and Cu in amorphous $Zr_{50}Ni_{50}$ [29] point to the fact that diffusion of Ni is faster than that of Cu by about an order of magnitude at these temperatures. This is supported by the observed size effects on diffusion in amorphous alloys [28, 30] suggesting that smaller atoms diffuse faster than bigger atoms in amorphous alloys. It thus appears from the above analysis that both Cu and Ni have moved beyond the oxide-alloy interface by several tens of nanometers after oxidation at 573 and 603 K. Figures 6 and 7 show depth profiles up to about 23–29 nm only and the oxide-alloy interface is not yet reached as evident from the plots. Due to practical difficulties encountered in experimentation, especially in increasing the sputtering rate, it was not possible to carry out the sputtering of the entire oxide film and thus to obtain an estimate of the oxide film thickness. Sun et al. reported oxide film thickness of about 60 nm formed on amorphous $Zr_{60}Al_{15}Ni_{25}$ after its oxidation in air at 603 K for 3 h and at 623 K for about 5 h [11]. It is thus likely that the oxide film thickness on the specimens of $Zr_{65}Cu_{17.5}Ni_{10}A_{17.5}$ in the present study might be of this order, i. e. about several tens of nanometers and the depth profiles in Fig. 6 originated from a part of the oxide film. However, the above analysis and interpretation of these depth profiles do provide valuable information about possible oxidation mechanisms for this alloy.

It is, thus, suggested from the above discussion that the depletion of Ni and Cu in the oxide film, as seen in Fig. 6, possibly arises due to their back diffusion into the alloy during oxidation of the alloy and the absence of these elements (Ni and Cu) in depth profiles after oxidation of the alloy specimen in the amorphous state can be understood. As the alloy reaches the supercooled liquid state during oxidation (at temperatures 633 and 663 K) strong segregation of Cu is noticed in the oxide film (Fig. 6) which point to a change in the mechanism of oxidation of the alloy in its supercooled liquid state, i.e. the oxidation mechanism is dominated by the inward diffusion of oxygen than the back diffusion of Ni and Cu into the alloy [11, 14]. During oxidation of the alloy the rate controlling process is

the back diffusion of Cu and Ni so long as the alloy remains in its amorphous state (which can be ascertained from the known T–T–T diagram of the alloy [17, 18] and it is most likely that Cu, being a slower diffuser than Ni, is present closer to the oxide-alloy interface than Ni and thus gets easily oxidized at 633 and 663 K when the alloy attains the supercooled liquid state after initial oxidation. This is evident from the plots shown in Figs. 2 and 6. In the supercooled liquid state the oxide film formation is dominated by the inward diffusion of oxygen anions and outward diffusion of cations of zirconium and copper. The diffusion rates of smaller atom (Cu here) are, in fact, about two orders of magnitude larger at temperatures of interest in the supercooled liquid state (633 and 663 K) than that in the amorphous state (573 and 603 K) [27–30]. This facilitates the outward diffusion of Cu and its consequent oxidation by inwardly moving oxygen atoms. Moreover, the larger amount of Cu (17.5 at.%) in the alloy than Ni (10 at.%) and the proximity of the former to the oxide-alloy interface after the initial oxidation till the alloy remained in the amorphous state are the favourable factors leading to the oxidation of Cu and the corresponding suppression of the oxidation of Ni in the supercooled liquid state of the alloy specimen. This explains the absence of Ni in depth profiles for oxidation of the alloy in the supercooled liquid state (Fig. 6). Some traces of Cu and Ni are seen (Figs. 2 and 3) on the as-received surface at 573 and 603 K (corresponding to the amorphous state) which possibly arise due to oxidation of some initial amount of Cu and Ni which was available just at the beginning of the oxidation process and these elements get subsequently depleted in the oxide layer and are possibly enriched near the oxide-alloy interface as the dominant rate controlling process for oxidation of the alloy in its amorphous state is their back-diffusion into the alloy. As a result no further presence of Cu or Ni is seen in the depth profiles of these elements in the oxide film formed on the alloy surface in its amorphous state (i.e. at 573 and 603 K).

Therefore, the observed trends of the depth profiles in Fig. 6 point to the role of Cu and Ni during the oxidation of the amorphous $Zr_{65}Cu_{17.5}Ni_{10}Al_{7.5}$ in air and support our previously proposed mechanism for oxidation of this alloy [14]. The change in diffusion mechanism at the glass transition temperature may likely be associated with the differences in the diffusion behaviour of smaller atoms (Cu and Ni) in the amorphous and the supercooled liquid states of the alloy [27, 28]. It is suggested from the above analysis that during oxidation in the amorphous state both Zr and Al having the most negative values of the heat of formation get preferentially oxidised with the rejection of Ni and Cu from the oxide film. Oxidation mechanisms suggested for this alloy are indeed consistent with the previously proposed mechanisms for air oxidation of similar type of alloys in the literature [11–13]. Sun et al. [11] during oxidation of amorphous $Zr_{60}Ni_{25}Al_{15}$ observed the absence of Ni in the oxide film formed on amorphous $Zr_{65}Ni_{25}Al_{15}$ after oxidation in air at temperatures below the glass transition temperature of the alloy. It was proposed [11] that Ni was rejected from the oxide film and its back diffusion into the alloy was the rate controlling process. The observations made in the present study also point to the fact that a similar mechanism appears to hold for oxidation of the amorphous $Zr_{65}Cu_{17.5}Ni_{10}Al_{7.5}$ in the amorphous state as suggested by Sun et al. [11] for the oxidation of the amorphous $Zr_{60}Ni_{25}Al_{15}$. It is noteworthy here that the oxidation of the alloy in amorphous and the supercooled liquid states was found to obey parabolic rate law with different activation energies in the respective states [14]. The observations of significant amount of Cu in the oxide films formed after oxidation in the supercooled liquid state clearly points to a different oxidation process. It is suggested that during oxidation in the supercooled liquid state the inward diffusion of oxygen becomes a dominant and the rate controlling process for the oxidation of the alloy in the supercooled liquid state. Triwikantoro et al. [12] and Koester and Trwikantoro [13] have suggested a similar mechanism for the oxidation of amorphous $Zr_{69.5}Cu_{12}Ni_{11}Al_{7.5}$ in air at 633 K for 4 h. It was mentioned in their investigation [13] that the alloy had a glass transition temperature of 635 K and the formation of some quasicrystals was noticed in the oxidised alloy specimen. It is very likely that the alloy oxidation did not correspond to the oxidation in the fully amorphous state and perhaps due to this reason no rejection of Ni and Cu was observed in their investigation and based on the results of their study it was suggested that the inward diffusion of oxygen was the dominant process for the growth of the oxide film on $Zr_{69.5}Cu_{12}Ni_{11}Al_{7.5}$. Therefore, the oxidation studies by Sun et al. $Zr_{60}Ni_{25}Al_{15}$ [11] and by Triwikantoro et al. [13] on $Zr_{69.5}Cu_{12}Ni_{11}Al_{7.5}$ are available evidences in the literature showing different oxidation mechanisms for high temperature air oxidation of a Zr–Cu–Ni–Al amorphous alloy depending on whether the alloy is fully amorphous or not. The results of our oxidation investigations carried out in air in the temperature range 573–663 K on $Zr_{65}Cu_{17.5}Ni_{10}Al_{7.5}$ also point to different type of oxidation processes for the alloy being in the amorphous or the supercooled liquid state during oxidation treatment.

In order to get some insight into the nature of oxide films formed on specimens oxidised in the amorphous and the supercooled liquid states, surface morphology of the oxide film was examined by SEM. Figures 8 and 9 represent surface morphologies obtained from specimens oxidised at two typical temperatures 603 K (corresponding to the amorphous state) and 663 K (corresponding to the supercooled liquid state). Figure 8 shows a relatively

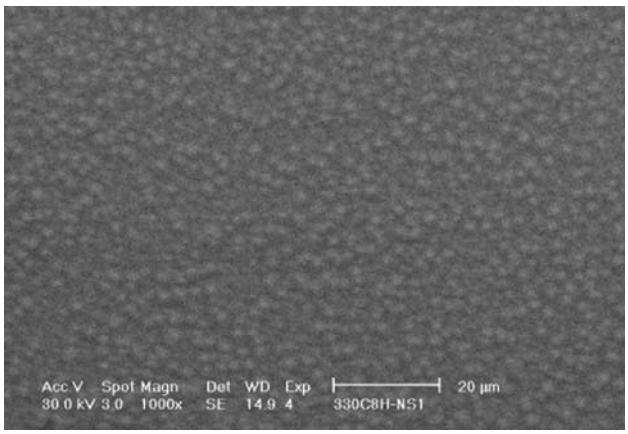

Fig. 8 Scanning electron micrograph of the oxide film formed on the amorphous $Zr_{65}Cu_{17.5}Ni_{10}Al_{7.5}$ after oxidation at 603 K for 3 h (alloy specimen in the amorphous state)

granular homogeneous distribution of oxidation products on the sample oxidised in its amorphous state at 603 K. On the other hand sample oxidised at 663 K (in its supercooled liquid state) showed a different morphology with some noticeable cracks in the oxide film. Such cracks have earlier been reported in the oxide films formed during oxidation of Zr–Ni amorphous alloys in air [7]. In fact, the presence of cracks in the oxide film formed at higher temperatures points to the presence of metallic species in oxidised forms. Cracks may have developed by expansion due to oxidation of metallic components into oxides, especially by the oxidation of Cu in the alloy under Zr-rich top layer. In fact, during the beginning of oxidation an initial Zr-rich oxide layer is already formed on the alloy specimen before it is transformed into its supercooled liquid state after short annealing time which can be ascertained from the known T–T–T diagram of the alloy [17, 18]. The high ratio between the volume of oxide and metal leads to a compressive stress in the oxide film resulting in a partial cracking of the oxide film. This is supported by the fact that the Pilling-Bedworth ratio of CuO, Cu_2O and ZrO_2 have values 1.73, 1.67 and 1.57, respectively [31]. These observations support our proposition that the rate kinetics for oxidation at higher temperatures (in supercooled liquid state) is dominated by inward diffusion of oxygen anions and outward diffusion of metal cations, especially of Zr and Cu [14].

Therefore, the observations reported in this study support the view that different oxidation mechanisms are operative for oxidation of the alloy $Zr_{65}Cu_{17.5}Ni_{10}Al_{7.5}$ at low temperatures (corresponding to the amorphous state of the alloy) and at high temperatures (corresponding to the supercooled liquid state of the alloy). It may, however, be argued that the change in mechanism could purely be a kinetic effect not being related to the change of structural state of the alloy. Though this possibility seems to be rather unlikely as the proposition for change in the oxidation mechanism was made on the basis of results obtained by study of oxidation kinetics of the alloy using the TGA [14] and the XPS analysis of the oxide films (present study), it may not be totally ruled out on the basis of the observations made in the present study. Further careful investigations to study the segregation/diffusion behaviour of Cu and Ni in the formation of oxide films at higher temperatures with much smaller oxidation times (e.g. permissible oxidation time is only 20 s at 633 K from the T–T–T diagram for the alloy $Zr_{65}Cu_{17.5}Ni_{10}Al_{7.5}$ [17, 18] so that the sample remains fully in the amorphous state in contrast to the oxidation time of 3 h used in the present study, which corresponds to the supercooled liquid state of the alloy) are required in order to unambiguously prove this point.

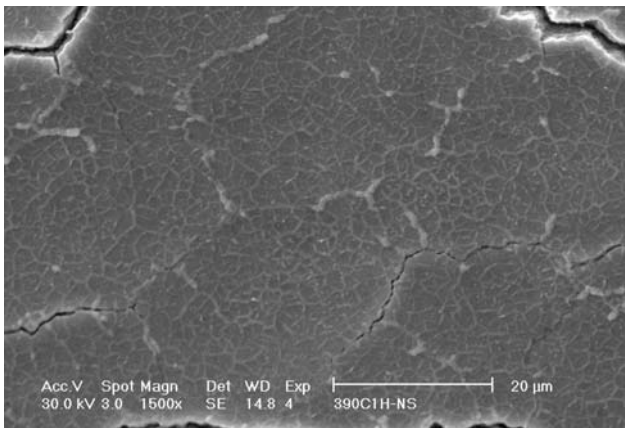

Fig. 9 Scanning electron micrograph of the oxide film formed on the amorphous $Zr_{65}Cu_{17.5}Ni_{10}Al_{7.5}$ after oxidation at 663 K for 3 h (alloy specimen in the supercooled liquid state)

Conclusions

The results of oxidation of the bulk amorphous alloy $Zr_{65}Cu_{17.5}Ni_{10}Al_{7.5}$ carried out in air in the temperature range 573–663 K revealed the following:

(1) The oxide film contained ZrO_2 as the major constituent along with some Al_2O_3 and CuO. Al_2O_3 was found in specimens oxidized at 573 and 603 K while CuO was present in specimens oxidized at 633 and 663 K. The observed depth profiles for Al and Cu suggest that the relative concentration of Al in the oxide films formed at 633 and 663 K becomes too low to yield a significant XPS peak due to Al as a result of strong segregation of Cu during oxidation at these temperatures.

(2) No Ni and Cu were detected in the oxide film formed at 573 and 603 K (corresponding to the amorphous state of the specimen) while appreciable amount of Cu (as CuO) was found in the oxide film formed at 633 and 663 K (corresponding to the supercooled liquid state). In the later case no Ni was detected due to strong segregation of Cu (Cu being present in much higher concentration in the alloy than Ni) and the proximity of Cu to the oxide–alloy interface.

(3) The above results are consistent with the previously proposed mechanism for the air oxidation of this alloy suggesting that the rate controlling process during the oxidation of the alloy at low temperatures (in the amorphous state) is the back diffusion of Ni and Cu while the oxidation at higher temperatures (in the supercooled liquid state) is dominated by the inward diffusion of oxygen and the outward diffusion of zirconium and copper.

Acknowledgements The financial support for this work from the Board of research in Nuclear Sciences (BRNS), Department of Atomic Energy (DAE), Government of India under the DAE/BRNS research Project (Grants No. 99/37/25/BRNS) is gratefully acknowledged. Thanks are due to Dr. K Raetzke for a critical reading of the manuscript and for many useful suggestions. The help provided by Ms Jugrita Zekonyte and Mr. Stefan Rehders during XPS measurement is gratefully acknowledged. Thanks are due to Dr. M. Sundararaman, Dr. J. G. Shah and Ms. M. S. Tawade from BARC, Mumbai for their help in recording SEM micrographs from oxidised alloy specimens.

References

1. Zhang T, Inoue A, Masumoto T (1991) Mater Trans JIM 32:1005
2. Johnson WL (1996) Curr Opin Solid State Mater Sci 1:383
3. Peker A, Johnson WL (1993) Appl Phys Lett 63:2342
4. Hashimoto K (1983) Amorphous metallic alloys. In: Luborsky FE (ed) Butterworths, London, p 471
5. Naka M, Hashimoto K, Masumoto T (1976) Corrosion 32:146
6. Dey GK, Savalia RT, Sharma SK, Kulkarni SK (1989) Corros Sci 29:823
7. Asami K, Kimura HM, Hashimoto K, Masumoto T (1995) Mat Trans JIM 36:988
8. Kiene M, Strunskus T, Hasse G, Faupel F (1999) Mater Res Soc Symp Proc. Materials Research Society, Pittsburgh, PA, USA, 554:167
9. Sharma SK, Strunskus T, Ladebusch H, Faupel F (2001) Mater Sci Eng A 304–306:747
10. Dhawan A, Raetzke K, Faupel F, Sharma SK (2001) Bull Mater Sci 24:281
11. Sun X, Schneider S, Geyer U, Johnson WL, Nicolet M-A (1996) J Mater Res 11:2738
12. Triwikantoro, Toma D, Meuris M, Koster U (1999) J Non-Cryst Solids 250–252:719
13. Koester U, Triwikantoro D (2001) Mater Sci Forum 360–362:29
14. Dhawan A, Raetzke K, Faupel F, Sharma SK, Phys Stat Sol (a) 199 No. 3 (2003) 431–438
15. Tam CY, Shek CH (2005) J Mater Res 20:1396
16. Kai W, Hsieh HH, Nieh TG, Kawamura Y (2002) Intermetallics 10:1265
17. Busch R (Private Communication)
18. Knorr K (1999) In: "Selbstdiffusion in Metallischen Massivglaesern". Ph. D Thesis, University of Muenster, Muenster, Germany
19. Wanger CD, Riggs WM, Davies LE, Moulder JF, Muilenberg GE (1979) Handbook of X-ray photoelectron spectroscopy. Perkin-Elmer, Eden Prairie, MN
20. Walz B, Oelhafen P, Guentherodt H-J, Baiker A (1989) Appl Surf Sci 37:337
21. Satoh H, Nakane H, Adachi H (1996) Appl Surf Sci 94/95:247
22. Betz G, Wehner GK (1983) Sputtering by particle bombardment II, vol 52. In: Behriech R (ed) Springer Verlag, Berlin, p 11
23. Malherbe JB, Hofmann S, Sanz JM (1986) Appl Surf Sci 27:355
24. Brundle CR, Chuang TJ, Wandelt K (1977) Surf Sci 68:459
25. Wandelt K (1982) Surf Sci Rep 2:75
26. "CRC handbook of chemistry and physics" (1995–96) 76th edn. Lide DR (ed) CRC Press, Boca Raton, pp 34–47
27. Knorr K, Macht M-P, Mehrer H (1999) Bulk metallic glasses. In: Johnson WL, Liu CT, Inoue A (ed) MRS symposia proceedings No. 554. Materials Research Society, Pittsburgh, p 269
28. Faupel F, Frank W, Macht M-P, Mehrer H, Naundorf V, Raetzke K, Schober HR, Sharma SK, Teichler H (2003) Revi Modern Phys 75:237
29. Hahn H, Averback RS, Shyu H-M (1988) J Less-Common Met 140:345
30. Sharma SK, Banerjee S, Kuldeep, Jain AK (1989) J Mater Res 4:603
31. Bradford SA (1990) In: ASM handbook, vol 13. ASM International, Materials Park, OH, p 64